Title

Human Rif1 protein binds aberrant telomeres and aligns along anaphase midzone microtubules.

Journal

The Journal of cell biology, 167(5)

ISSN

0021-9525

Authors

Xu, Lifeng
Blackburn, Elizabeth H

Publication Date

2004-12-01

DOI

10.1083/jcb.200408181

Peer reviewed

Human Rif1 protein binds aberrant telomeres and aligns along anaphase midzone microtubules

Lifeng Xu and Elizabeth H. Blackburn

Department of Biochemistry and Biophysics, University of California, San Francisco (UCSF), San Francisco, CA 94143

We identified and characterized a human orthologue of Rif1 protein, which in budding yeast interacts in vivo with the major duplex telomeric DNA binding protein Rap1p and negatively regulates telomere length. Depletion of hRif1 by RNA interference in human cancer cells impaired cell growth but had no detectable effect on telomere length, although hRif1 overexpression in *S. cerevisiae* interfered with telomere length control, in a manner specifically dependent on the presence of yeast Rif1p. No localization of hRif1 on normal human telomeres, or interaction with the human telomeric proteins TRF1, TRF2, or hRap1, was detectable. However, hRif1 efficiently translocated to telomerically located DNA damage foci in response to the synthesis of aberrant telomeres directed by mutant-template telomerase RNA. The hRif1 level rose during late S/G2 but hRif1 was not visible on chromosomes in metaphase and anaphase; however, notably, specifically during early anaphase, hRif1 aligned along a subset of the midzone microtubules between the separating chromosomes. In telophase, hRif1 localized to chromosomes, and in interphase, it was intranuclear. These results define a novel subcellular localization behavior for hRif1 during the cell cycle.

Introduction

Telomeres are the protective structures at the ends of eukaryotic chromosomes that prevent chromosome termini from undergoing unregulated degradation, recombination, and fusion. They are specialized nucleoprotein complexes that consist of tandemly repeated DNA sequences bound by various telomeric proteins (Blackburn, 2001). Three different types of telomere-associated proteins have been described: double-stranded telomeric DNA binding proteins and their associated factors; single-stranded telomeric DNA binding proteins and their associated factors; and certain components of the general DNA damage response pathways that also localize at telomeres (Blackburn, 2001; Smogorzewska and De Lange, 2004).

Telomeres are maintained at well-controlled lengths by factors that work to either lengthen or degrade telomeric DNA. In most organisms, the telomeric repeat tracts are synthesized by telomerase (Greider and Blackburn, 1985). The core components of telomerase, a ribonucleoprotein complex, include a reverse transcriptase and an RNA moiety that contains a short template sequence for the telomeric DNA repeats (Blackburn, 2000). Proper telomere maintenance requires not only telomerase activity but also the telomere-associated factors, which maintain telomere length homeostasis by regulating telomerase recruitment, and the accessibility of telomeres to telomerase as well as to exonucleases that act to degrade telomeres (Blackburn, 2001; Smogorzewska and De Lange, 2004).

From budding yeast to human cells, different sets of duplex telomeric DNA repeat–binding factors and their interacting proteins have been identified and characterized. Although much divergence has occurred in these proteins across species, there are also significant levels of conservation. In budding yeasts such as *S. cerevisiae*, the telomeric protein Rif1p interacts in vivo with Rap1p, the major telomeric double-stranded DNA binding protein (Hardy et al., 1992; Wotton and Shore, 1997). Rap1p also interacts with Rif2p in vivo, and mutations of Rap1p disrupting its Rif1p and Rif2p binding, as well as deletions of Rif1p and Rif2p proteins themselves, cause significant telomere lengthening (Wotton and Shore, 1997). The Rif proteins can also negatively regulate telomere length independent of their recruitment by Rap1p (Levy and Blackburn, 2004).

In the fission yeast *S. pombe*, duplex telomeric DNA repeats are bound by Taz1p, a homologue of the human TRF proteins (Cooper et al., 1997), and *S. pombe* orthologues of *S. cerevisiae* Rap1p and Rif1p have been identified (Chikashige and Hiraoka, 2001; Kanoh and Ishikawa, 2001). spRap1p does not directly bind to telomeric DNA and is apparently recruited there by Taz1p. Although the *S. pombe* Rif1p negatively regulates

The online version of this article contains supplemental material.

Correspondence to Elizabeth H. Blackburn: telomer@itsa.ucsf.edu

Abbreviation used in this paper: RACE, rapid amplification of cDNA ends.

The Journal of Cell Biology, Vol. 167, No. 5, December 6, 2004 819–830
http://www.jcb.org/cgi/doi/10.1083/jcb.200408181

telomere length and is found by ChIP analysis to be enriched at telomeres, it differs from *S. cerevisiae* Rif1p in several aspects. First, it interacts with Taz1p instead of spRap1p in a two-hybrid assay. Second, immunostaining shows that it localizes heterogeneously in the nucleus in wild-type cells and was only seen to translocate to telomeres after depletion of spRap1.

Although there is a human Rap1 orthologue (hRap1) which localizes at telomeres and regulates telomere length like *S. pombe* Rap1p, it does not bind human telomeric DNA by itself in vitro (Li et al., 2000; Li and de Lange, 2003). Instead, hRap1 interacts in a yeast two-hybrid assay with TRF2 (Li et al., 2000). TRF2 is one of two structurally related telomeric proteins, TRF1 and TRF2, that each directly binds duplex human telomere repeats (Broccoli et al., 1997). Removal of TRF2 from telomeres by expressing a dominant negative allele of TRF2 results in the loss of hRap1 at telomeres (Li et al., 2000). Thus, hRap1 has apparently no detectable telomeric DNA binding capability and is thought to be tethered to telomeres through its interaction with TRF2.

Here, we describe the identification and characterization of a human Rif1 orthologue. We report that although the hRif1 protein does not detectably localize at normal telomeres, nor interact with TRF1, TRF2, or hRap1, it can translocate to aberrant telomeres synthesized under the direction of a telomerase RNA template mutant. Consistent with a recent report (Silverman et al., 2004), hRif1 similarly colocalizes to chromosomal-wide sites of MMS-induced damage. Hence, hRif1 protein can localize to DNA damage foci in response to both general and telomere-specific chromosomal aberrancies. We also report that during the cell cycle, hRif1 shows a novel subcellular distribution pattern: hRif1 becomes associated with chromatin at telophase, but is absent from chromosomes in metaphase and anaphase. Significantly, hRif1 aligns along a subset of the midzone microtubules in early anaphase. Hence, we suggest that hRif1 might also be involved in regulating microtubule structures at mitosis, possibly through modulation of microtubule properties to help monitor appropriate chromosome segregation in mitosis.

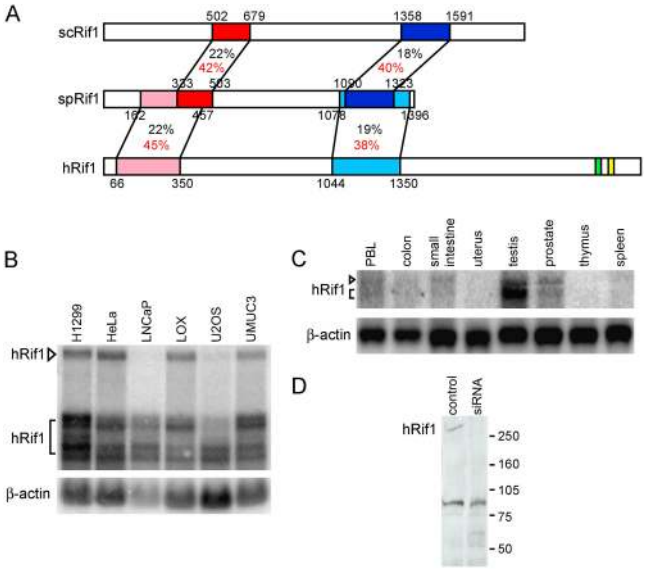

Figure 1. **Sequence conservation and expression of hRif1.** (A) Schematic representation of sequence similarities of Rif1 proteins. Percentage identities are in black and percentage similarities are in red. A putative NLS is marked in green. The alternatively spliced-out peptide of hRif1 is marked in yellow. (B) Ubiquitous expression of hRif1 mRNA in human cancer cell lines. 2 μg of mRNAs from different cell lines were treated with glyoxal, electrophoresed on a 20 cm × 25 cm 0.8% agarose gel, transferred to a Hybond NX membrane and hybridized with hRif1 or β-actin cDNA probes. The bracket and arrowhead indicate groups of alternatively spliced hRif1 mRNAs. (C) Expression of hRif1 mRNA in adult human tissues. A multiple tissue Northern blot (CLONTECH Laboratories, Inc.) was hybridized with hRif1 or β-actin cDNA probes. Separation of alternatively spliced hRif1 mRNA was not as clear as in B because the mRNA electrophoresis was performed in a much smaller (6 cm × 8 cm) 1% agarose gel. The bracket and arrowhead indicate the groups of hRif1 mRNAs corresponding to those indicated in B. (D) Immunoblot of hRif1 protein with antibody PAB2857. LOX cells were infected with lentiviruses expressing siRNA sequences targeting hRif1 mRNA. 3 d after infection, 50 μg of whole cell extracts were analyzed by Western blot analysis and probed with PAB2857.

Results

Cloning of hRif1

We identified a human orthologue of the yeast telomeric protein Rif1 (Fig. 1 A). A partial human EST sequence that shares sequence homology with the NH_2-terminal region of the *S. cerevisiae* and *S. pombe* Rif1p was reported previously (Kanoh and Ishikawa, 2001). We assembled a full-length hRif1 cDNA by homology alignment with the partial sequence, exon prediction from genomic sequences, and 5′- and 3′-rapid amplification of cDNA ends (RACE). The full-length cDNA was then cloned by RT-PCR. Multiple alternatively spliced forms of the 5′-untranslated region were detected by the 5′-RACE analyses. However, they all conform to the same initiator ATG sequence. The ORF of the cDNAs encodes a protein of 2,472 aa. A COOH-terminal region of the cDNA encoding 26 aa is alternatively spliced out, resulting in a 2446–amino acid form (Fig. S1, available at http://www.jcb.org/cgi/content/full/jcb.200408181/DC1). RT-PCR from different human cancer cell lines demonstrated that the mRNA encoding this shorter protein product was much more abundant than that encoding the longer product (unpublished data). Sequence analysis of the hRif1 protein shows that it shares sequence homology to *S. cerevisiae* and *S. pombe* Rif1 at both NH_2- and COOH-terminal regions (Fig. 1 A) but contains no known protein motifs. Northern blotting analysis showed that the hRif1 mRNA is ubiquitously expressed and alternatively spliced in various human cancer cell lines, but the major size differences of alternatively spliced mRNA all occurred outside the protein coding region (Fig. 1 B and Fig. 2 A). Multiple-tissue Northern blots demonstrated that the hRif1 mRNA is highly expressed in testis but is at very low levels in thymus and uterus (Fig. 1 C), which is consistent with the expression pattern of a mouse Rif1 orthologue reported recently (Adams and McLaren, 2004).

Cellular effects of hRif1 depletion by siRNA

RIF1 gene deletion in *S. cerevisiae* leads to substantially longer telomeres but generally normal cell growth (Wotton and Shore,

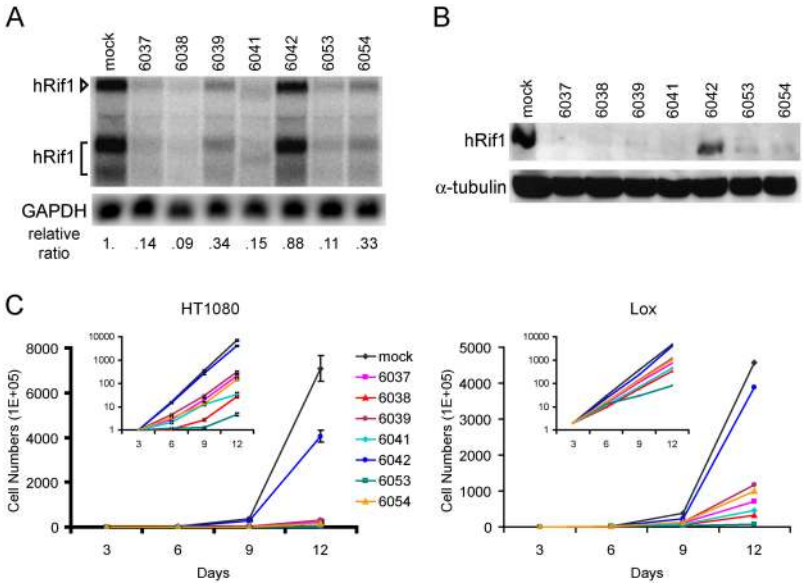

Figure 2. **Impaired cell growth upon depletion of hRif1.** (A) Knockdown of hRif1 mRNA levels by siRNA treatment. LOX cells were infected with lentiviruses expressing hairpin siRNAs against different sequences within the protein coding region of hRif1 mRNA. 2 d after infection, 40 μg of total RNA from each cell line was hybridized with hRif1 or GAPDH probes. Relative hRif1 levels were determined by ImageQuant software using GAPDH as the loading control. (B) Depletion of hRif1 protein levels by siRNA. 50 μg of whole cell extracts from each cell line were probed with PAB2857 and α-tubulin antibodies. siRNA treatment was performed as described in A. (C) hRif1 depletion leads to cell growth inhibition in HT1080 and LOX cells. HT1080 cells and LOX cells were infected with lentiviral siRNA constructs at >95% efficiencies, as indicated by a GFP expressed from the same lentiviral vector. Cell numbers were counted every 3 d after infection and cell counts are shown as mean ± SD of plates analyzed in triplicate.

1997). To test the cellular effects of hRif1 depletion we stably knocked down hRif1 expression in tissue culture human cancer cells and examined both cell growth and telomere length maintenance. We used a lentiviral delivery and expression system (Li et al., 2004) to express hairpin siRNAs directed against several different regions of the hRif1 mRNA (see Materials and methods). As shown in Fig. 2 (A and B), six of the seven siRNA constructs tested knocked down hRif1 expression to varying extents. With both melanoma LOX cells and fibrosarcoma HT1080 cells, we observed that cells with suppressed levels of hRif1 grew significantly slower than the control cells, whereas the siRNA sequence (construct 6042) that barely decreased the hRif1 mRNA level had little effect on cell growth (Fig. 2 C). The effects on cell growth correlated generally well with the degrees of hRif1 knockdown with the different siRNAs tested. We passaged these cells continuously in medium selective for the lentiviral siRNA constructs for over 120 d and examined telomere length by Southern blotting analysis. Unlike in *S. cerevisiae*, in which deletion of *scRif1* results in longer telomeres (Hardy et al., 1992), no significant differences in telomere length were detected in cell lines depleted of hRif1 compared with the mock-infected cells (Fig. S2, available at http://www.jcb.org/cgi/content/full/jcb.200408181/DC1).

Association of hRif1 with aberrant telomeres

It has been demonstrated that at least a subset of *S. cerevisiae* Rif1p protein colocalizes with scRap1p protein at telomeres by immunofluorescence staining (Mishra and Shore, 1999; Smith et al., 2003). To examine hRif1 localization, we developed affinity-purified rabbit pAbs against peptides aa 2106–2123 and aa 2457–2472 of hRif1 (PAB2852 and PAB2857, respectively). We note that the two peptide antibodies used in the work recognize peptide sequences outside the alternatively spliced region (Fig. 1 A and Fig. S1) and thus will recognize both the longer (2472 aa) and the more abundant shorter (2446 aa) hRif1 proteins. For simplicity, in the paper we refer to hRif1 to include both the longer and the shorter hRif1 protein forms. Immunoblotting of whole cell extracts from control cells and cells depleted of hRif1 by siRNA verified that both antibodies recognized hRif1 (Fig. 1 D; not depicted). Immunostaining of tissue culture cells with each antibody showed heterogeneous nuclear staining, but no evidence of the punctate nuclear telomeric spots characteristic of TRF1, TRF2, or hRap1 staining (Fig. 3 B, top). In addition, to examine whether any fraction of hRif1 associates with known telomere binding proteins, coimmunoprecipitation experiments were performed between hRif1 and TRF1, TRF2 and hRap1 in multiple tissue culture cell lines. Unlike the mouse Rif1 which was recently reported to associate with mouse TRF2 (Adams and McLaren, 2004), no significant interactions were detected between Rif1 and TRF2, TRF1, or hRap1 (see Materials and methods; unpublished data). Together, these data suggest that hRif1 does not localize to normal human telomeres.

Kanoh and Ishikawa (2001) reported that in *S. pombe* Rif1p protein stained heterogeneously in the nucleus, but moved to telomeres when *spRap1* gene was deleted. We considered the possibility that the SpRap1p depletion caused telomere uncapping. For simplicity, the term telomere uncapping is used in this work to refer to telomeres with different types and degrees of abnormalities induced by the various methods specified in each context discussed. Such uncapping could have led the translocation of SpRif1p to the resulting aberrant telomeres. Therefore, we tested whether hRif1 localization in LOX and HeLa human cancer cell lines was affected by uncapping telomeres in different ways. Overexpression of a dominant negative form of TRF2 has previously been reported to cause depletion of telomere-associated TRF2 and telomere uncapping (Karlseder et al., 1999; Takai et al., 2003), so we first attempted to uncap telomeres either by siRNA-mediated depletion of the telomere binding proteins TRF1, TRF2, or hRap1 (Fig. 3, A and B). We also uncapped telomeres by expressing a telomerase RNA template mutant (MT-hTer) that directs synthesis of deleterious telomeric repeats to the extreme tips of the

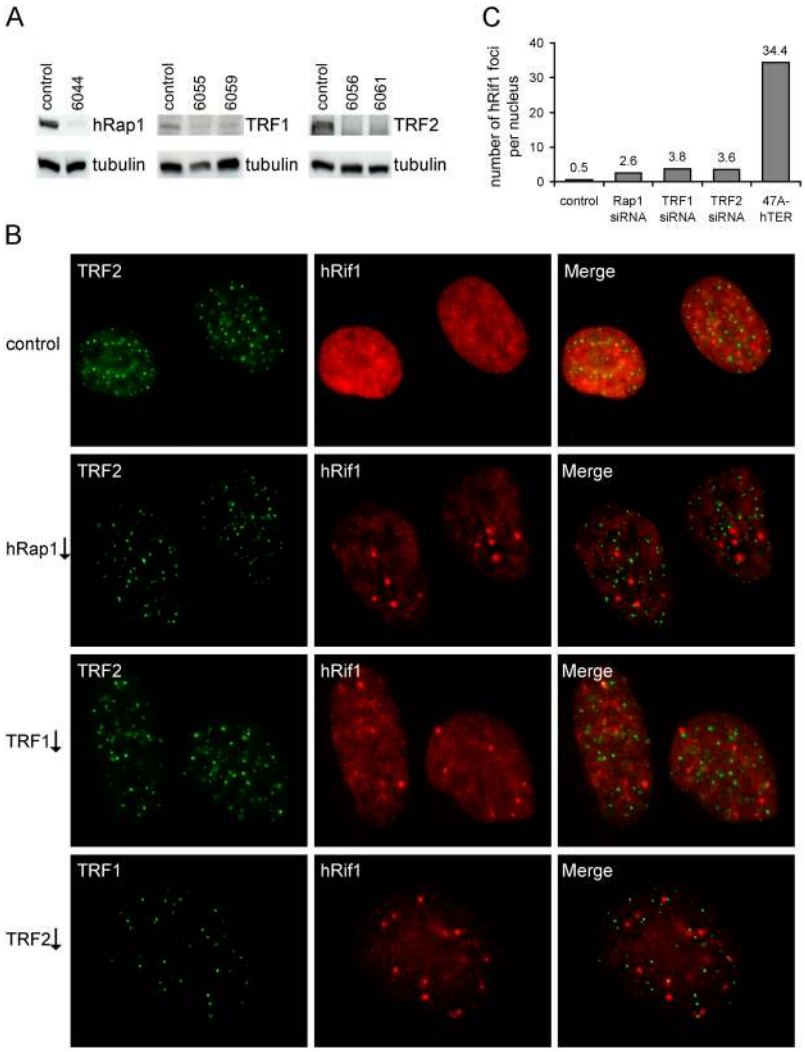

Figure 3. **No detectable localization of hRif1 protein at telomeres in normal cells or in cells depleted of hRap1, TRF1, or TRF2 protein.** (A) Western blot analysis of whole cell extracts from LOX cells treated with lentiviruses expressing hairpin siRNAs against TRF1, TRF2, or hRap1. (B) Immunofluorescence analysis of hRif1 protein in LOX melanoma cells. LOX cells were infected with lentiviruses expressing hairpin siRNAs against hRap1, TRF1, or TRF2. 3 d after infection, cells were fixed and stained with hRif1 antibody PAB2857 (red) and TRF1 or TRF2 antibodies (green). A microscope (model Eclipse E600; Nikon) with a 100× objective and a Coolsnap *fx* charge-coupled device camera and software (Roper Scientific) was used to visualize the image. (C) Histogram showing the average numbers of hRif1 foci per nucleus in LOX cells after treatment with lentiviruses expressing hairpin siRNAs against hRap1, TRF1, TRF2, or with lentiviruses expressing hTER template mutant 47A. For each treatment, hRif1 foci in ~50 interphase cells were counted after immunofluorescence analysis and the average numbers per nucleus were presented.

telomeric repeat tracts (Kirk et al., 1997; Marusic et al., 1997). After each treatment, we examined hRif1 localization.

In both LOX and HeLa cells, TRF1 and TRF2 depletion each induced significant amounts of cell apoptosis, whereas hRap1 depletion had little effect on cell growth (unpublished data). We performed dual immunostaining of hRif1 and telomere binding proteins TRF1 or TRF2 3 d after the introduction of each siRNA in LOX cells and HeLa cells (i.e., after ~3 cell population doublings; Fig. 3, A and B; not depicted). Although by day 3 the cells infected with lentiviruses expressing hRap1, TRF1, or TRF2 siRNA had increased numbers of hRif1 foci per nucleus (mean numbers of 2.6, 3.8, and 3.6, respectively, vs. 0.5 foci/nucleus in mock-infected control cells; 50 cells were counted in each staining; Fig. 3, B and C), these foci seldom colocalized with telomeres.

As an independent way of uncapping telomeres, we introduced a lentiviral vector expressing a telomerase template mutant, MT-hTer-47A (Li et al., 2004), in LOX and HeLa cells. This mutant telomerase RNA synthesizes mutant telomeric repeats (Marusic et al., 1997; Li et al., 2004) that are predicted to have lost binding affinity for TRF1 and -2. The control was cells infected in parallel with a lentiviral expression vector expressing wild-type telomerase RNA (WT-hTER). hRif1 localization was then examined via deconvolution microscopy. In these control cells, the hRif1 staining pattern was indistinguishable from that of the mock-infected cells (unpublished data). In contrast, in cells expressing 47A-hTer, hRif1 accumulated in numerous distinct nuclear foci (mean number 34.4 foci per cell; Fig. 3 C and Fig. 4 A). To investigate the nature of the foci, we first performed coimmunostaining of hRif1 with antibody against TRF2. TRF2 protein specifically localizes at human telomeres (Broccoli et al., 1997). As shown in Fig. 4 A, the majority of hRif1 foci localized at or near telomeres. Because uncapped telomeres can elicit cellular responses similar to damaged DNA (Takai et al., 2003; Li et al., 2004), we then performed dual staining of hRif1 with the DNA damage response protein 53BP1. 53BP1 is known as a mediator of DNA damage signaling; upon DNA damage, 53BP1 is recruited rapidly to sites of DNA double-strand breaks and forms discrete nuclear foci (Schultz et al., 2000; Rappold et al., 2001). As shown in Fig. 4 B, expression of hTER template mutant 47A induced numerous 53BP1 foci in the nucleus. Almost all the 53BP1 foci overlapped with the hRif1 foci in these cells, indicating that hRif1 localized at aberrant telomeres to produce

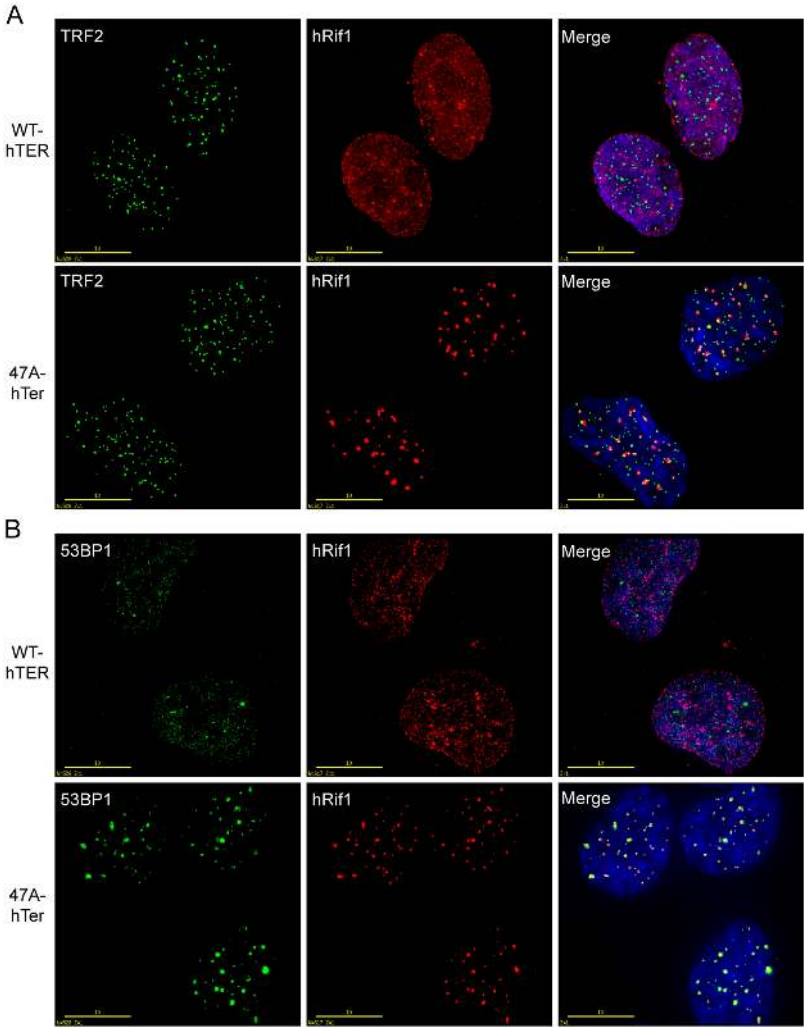

Figure 4. **hRif1 accumulation on uncapped telomeres synthesized by hTER template mutant 47A.** Images were analyzed with a Deltavision microscopy system using the Deltavision SoftWorx resolve3D capture program and collected as a stack of 0.2-μm increments in the z axis. After deconvolution, images were viewed with the Quick Projection option. (A) hRif1 protein translocates to telomeres upon expression of hTER template mutant 47A (47A-hTer). LOX cells were infected with lentiviruses expressing wild-type hTER (WT-hTER) or 47A-hTer. 3 d after infection, cells were fixed and stained with TRF2 antibody (green), hRif1 antibody PAB2852 (red), and DAPI (blue). (B) hRif1 foci overlap with 53BP1 foci in LOX cells expressing 47A-hTer. Lentiviral infections were performed as described in A. Cells were stained with 53BP1 antibody (green), hRif1 antibody (red), and DAPI (blue). Bars, 10 μm.

foci like those known to accumulate at DNA damage sites. Dual staining with antibody against phosphorylated ATM protein (Bakkenist and Kastan, 2003), another early DNA damage response sensor, and with antibody against hRif1 showed similar colocalization results (unpublished data).

We conclude that unlike *S. cerevisiae* Rif1p, hRif1 protein does not associate with telomeres under normal conditions. However, upon expression of a telomerase template mutant, hRif1 and other DNA damage response factors efficiently translocate to aberrant telomeres, suggesting that a significant portion of the telomeres became uncapped and resembled DNA damage after the mutant-template telomerase RNA expression. Various reasons may account for why we did not detect significant hRif1 localization at telomeres depleted of TRF1, TRF2, or hRap1 by siRNA treatment. First, the degrees of depletion of the aforementioned telomere binding factors (Fig. 3 A) might not have been enough to induce significant telomere damage. Second, depletion of the total levels of hRap1, TRF1, or TRF2 by RNA interference might have induced a cellular response different from the telomere aberrancy that was induced by incorporation of mutant telomeric repeats or by expression of a dominant negative TRF2. This interpretation is consistent with a previous report showing a much milder increase in telomere associated DNA damage foci induced by siRNA-mediated TRF2 depletion compared with that induced by expression of a dominant negative TRF2 (Takai et al., 2003). We suggest that when TRF1, TRF2, and hRap1 proteins were depleted by RNA interference, the appearance of more hRif1 foci (most of which were not at telomeres but colocalized with 53BP1; Fig. 3 B and not depicted) might represent sites of chromosomal DNA breaks caused by telomere fusions (known to be induced by TRF2 depletion from telomeres; van Steensel et al., 1998) followed by anaphase bridging and consequent chromosome breakage.

It has been demonstrated that telomeres deficient in TRF2 binding induce a p53-dependent apoptotic response (Karlseder et al., 1999). To explore the role of p53 in the response of hRif1 to mutant-sequence telomeres, we expressed telomerase RNA template mutant 47A in two human colon cancer cell lines that are isogenic except for their p53 status, HCT116 (p53WT) and HCT116 (p53−/−) (Bunz et al., 1998). Indirect immunofluorescence staining demonstrated that hRif1 translocated to discrete DNA damage foci as indicated by 53BP1 accumulation upon expression of template mutant 47A in both cell lines with similar efficiency (Fig. 5). This result indicated that hRif1 can respond to damaged telomeres without a requirement for p53.

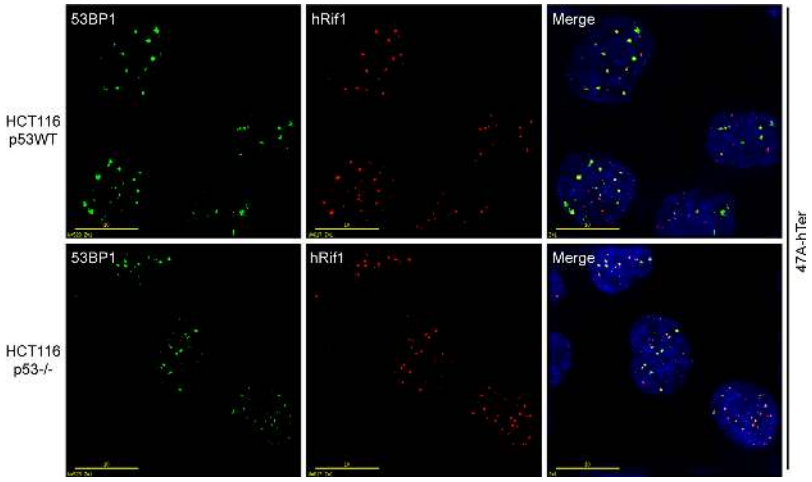

Figure 5. **hRif1 localizes on uncapped telomeres without a requirement for wild-type p53.** HCT116 cell lines with the p53 locus wild type or disrupted, but which were otherwise isogenic, were infected with lentiviruses expressing 47A-hTer. 5 d after infection, cells were fixed and stained with 53BP1 antibody (green), hRif1 antibody PAB2852 (red), and DAPI (blue). Images were acquired with a Deltavision microscopy system as described for Fig. 4. Bars, 10 μm.

hRif1 overexpression in *S. cerevisiae* interferes with telomere length maintenance

Having shown that human Rif1 can localize to telomeres when they are made aberrant, we further investigated any potential telomeric role of hRif1 by testing whether the protein retains any evolutionarily conserved functional property across species. Because *S. cerevisiae* Rif1p and Rif2p negatively regulate telomere length (Wotton and Shore, 1997), we examined the effect of hRif1 overexpression on telomeric tract length in *S. cerevisiae* in wild-type yeast cells and in cells deleted for the *scRif1* gene, *scRif2* gene, or both. The hRif1 full-length cDNA was cloned into a yeast 2μ-plasmid under the control of the ADH1 promoter and transformed into a *RIF1/rif1*, *RIF2/rif2* heterozygous *S. cerevisiae* strain. The empty vector was used as a control. The resulting strains were sporulated and spores with desired genotypes overexpressing hRif1 or vector alone were selected and passaged on plates consecutively for five streaks (~125 population doublings) to allow telomere length to reach equilibrium. We then compared the effects of human Rif1 overexpression in the wild-type, Δ*rif1*, Δ*rif2* and Δ*rif1*Δ*rif2* mutant yeast cells. Data from five independent sporulation experiments showed that overexpression of hRif1 in wild-type and Δ*rif2* strains led to significant telomere elongation; mean telomere length averaged 330 and 910 bp longer, respectively. In contrast, overexpression of hRif1 in Δ*rif1* or Δ*rif1*Δ*rif2* strains did not induce significant telomere length changes compared with the vector control (changes ≤120 bp; Fig. 6, A and B; Fig. S3, available at http://www.jcb.org/cgi/content/full/jcb.200408181/DC1). The finding that hRif1 overexpression perturbs telomere length maintenance, in a manner specifically dependent on the presence of the *S. cerevisiae Rif1* gene, suggests that hRif1 and scRif1p proteins share at least some conserved functional interactions that can directly or indirectly affect telomeres.

hRif1 is involved in the DNA damage response

It has recently been reported that hRif1 localizes to sites of general DNA damage (Silverman et al., 2004). To confirm that hRif1 plays a role in the general DNA damage response in the human cell lines used in this work, we induced DNA damage in LOX cells by treating the cells with MMS. Immunostaining of endogenous hRif1 protein after MMS treatment for 1 h revealed a punctate nuclear pattern for hRif1. Co-staining with antibody against 53BP1 confirmed that these hRif1 foci colocalized with 53BP1 (Fig. 7 A). The appearance and size of these hRif1 foci was reminiscent of the telomerically located foci that had been induced by the 47A mutant-template telomerase RNA expression as described above. To verify independently that the punctate nuclear pattern is specific to hRif1 protein, we also transfected LOX cells with a GFP-hRif1 fusion protein expression construct and then subjected the cells to the same 1-h MMS treatment. As shown in Fig. 7 B, GFP-hRif1 protein distributed heterogeneously in the nucleus in control cells, whereas after MMS treatment, GFP-hRif1 protein trans-

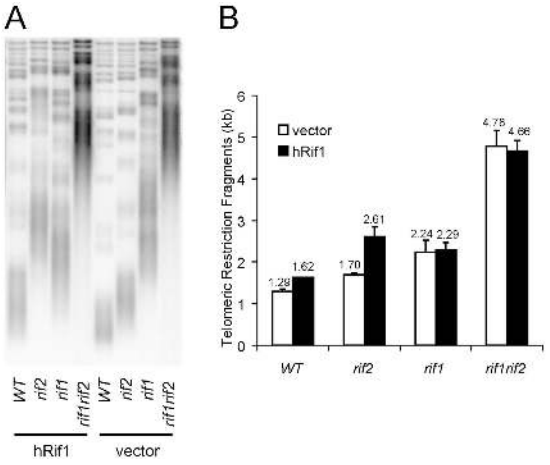

Figure 6. **hRif1 overexpression in *S. cerevisiae* perturbs telomere length maintenance dependent on the presence of the *scRif1* gene.** (A) Southern blot of telomeric restriction fragments in wild-type, Δ*rif1*, Δ*rif2*, and Δ*rif1*Δ*rif2* mutant yeast cells overexpressing hRif1 or the vector-alone control. Genomic DNA was isolated from yeast cells, digested with XhoI, and hybridized with a telomeric probe. (B) Histogram of bulk telomeric restriction fragments in wild-type, Δ*rif1*, Δ*rif2*, and Δ*rif1*Δ*rif2* mutant yeast cells overexpressing hRif1 or the vector-alone control. Length of peak telomeric restriction fragments was quantified with ImageQuant from five independent sporulation experiments and is shown as mean ± SD.

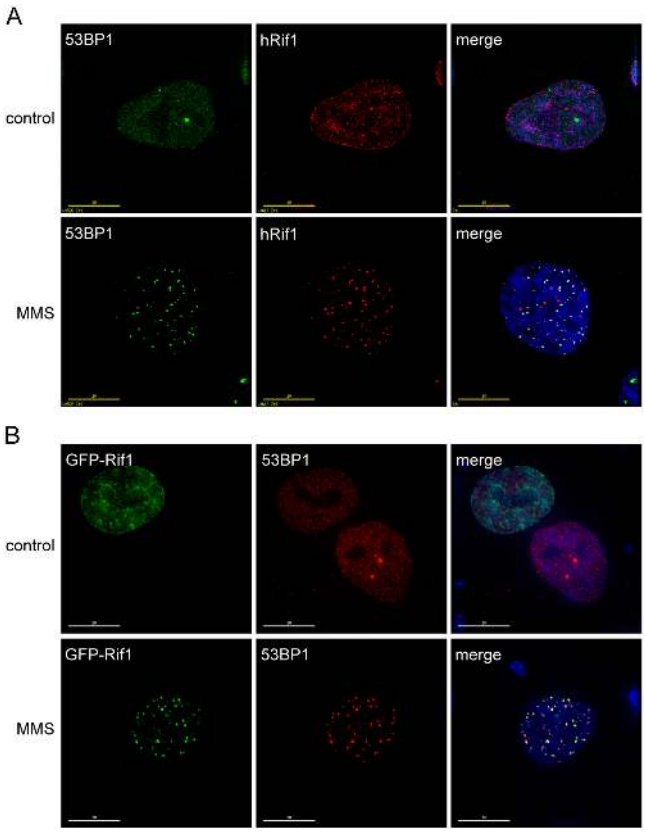

Figure 7. **Accumulation of hRif1 protein at DNA damage foci induced by MMS treatment.** Images were acquired with a Deltavision microscopy system as described for Fig. 4. (A) LOX cells were treated with 0.01% MMS for 1 h, then fixed and immunostained with 53BP1 antibody (green) to visualize DNA damage foci, hRif1 antibody PAB2852 (red) to visualize the endogenous hRif1 protein, and DAPI (blue). (B) GFP-hRif1 fusion protein localizes to DNA damage foci induced by MMS treatment. LOX cells were transfected with pEGFP-hRif1 expression construct. 2 d after transfection, cells were treated with 0.01% MMS for 1 h, fixed and stained with 53BP1 antibody (red) and DAPI (blue). Bars, 10 μm.

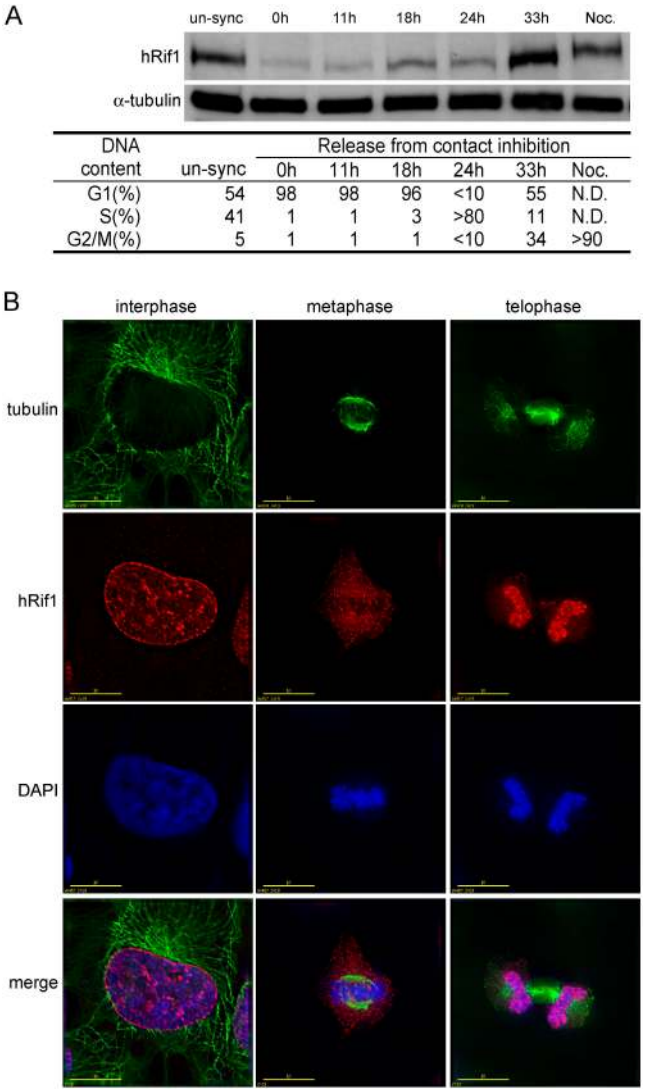

DNA content	un-sync	Release from contact inhibition 0h	11h	18h	24h	33h	Noc.
G1(%)	54	98	98	96	<10	55	N.D.
S(%)	41	1	1	3	>80	11	N.D.
G2/M(%)	5	1	1	1	<10	34	>90

Figure 8. **Cell cycle–regulated expression and intracellular distribution of hRif1 protein.** (A) hRif1 protein levels are regulated across the cell cycle. Contact-inhibited T24 cells were released into the cell cycle for 0–33 h, as indicated above the lanes. Whole cell extracts were probed with hRif1 antibody PAB2857 or α-tubulin antibody. DNA contents of synchronized cells at different time points were determined by FACS analysis. Noc., cells were released into the cell cycle for 28 h and then treated with 0.3 μg/ml nocodazole for 10 h for a M phase block. (B) hRif1 dynamically associates with chromatin during the cell cycle. LOX cells were fixed and immunostained with β-tubulin antibody (green), hRif1 antibody (red), and DAPI (blue). Images were analyzed with a Deltavision microscopy system using the Deltavision SoftWorx resolve3D capture program and collected as a stack of 0.2-μm increments in the z axis. After deconvolution, an image of a representative single section on the z axis saved as a Photoshop file is presented. Bars, 10 μm.

located to discrete foci that overlapped with 53BP1 protein. These data confirm that hRif1 plays a role in the response to general DNA damage. Hence, we suggest that the translocation of hRif1 to aberrant telomeres that we have observed reflects its role in a DNA damage response at uncapped telomeres.

Cell cycle–dependent levels and intracellular distribution of hRif1

In *S. cerevisiae*, *Rif1* gene transcription displays periodic fluctuation through the cell cycle, peaking during S phase (Cho et al., 1998). In addition, scRif1p protein association with telomeric chromatin changes during the cell cycle; being minimal at the beginning of S and G1 phase and maximal at mid/late S and G2 phase, and decreasing around mitosis (Smith et al., 2003). To further our understanding of hRif1, we examined both the protein level and intracellular localization of hRif1 across the cell cycle.

To investigate whether hRif1 protein expression varies during the cell cycle, we measured hRif1 protein steady-state levels by Western blot analysis using synchronized populations of T24 human bladder carcinoma cells. Parallel cultures of T24 cells were arrested at G0/G1 by contact inhibition. Cells were then released from arrest by replating them at low density in fresh medium (Chen et al., 1996). The cell-cycle distribution profile of the synchronized culture at each time point was determined by FACS analysis of DNA content. As shown in Fig. 8 A, hRif1 protein levels were low in G0, G1, and S phase, but rose in G2/M phase. In cells arrested in M phase by nocodazole treatment for 10 h, hRif1 accumulated at intermediate levels (Fig. 8 A). The periodic variations of hRif1 protein expression

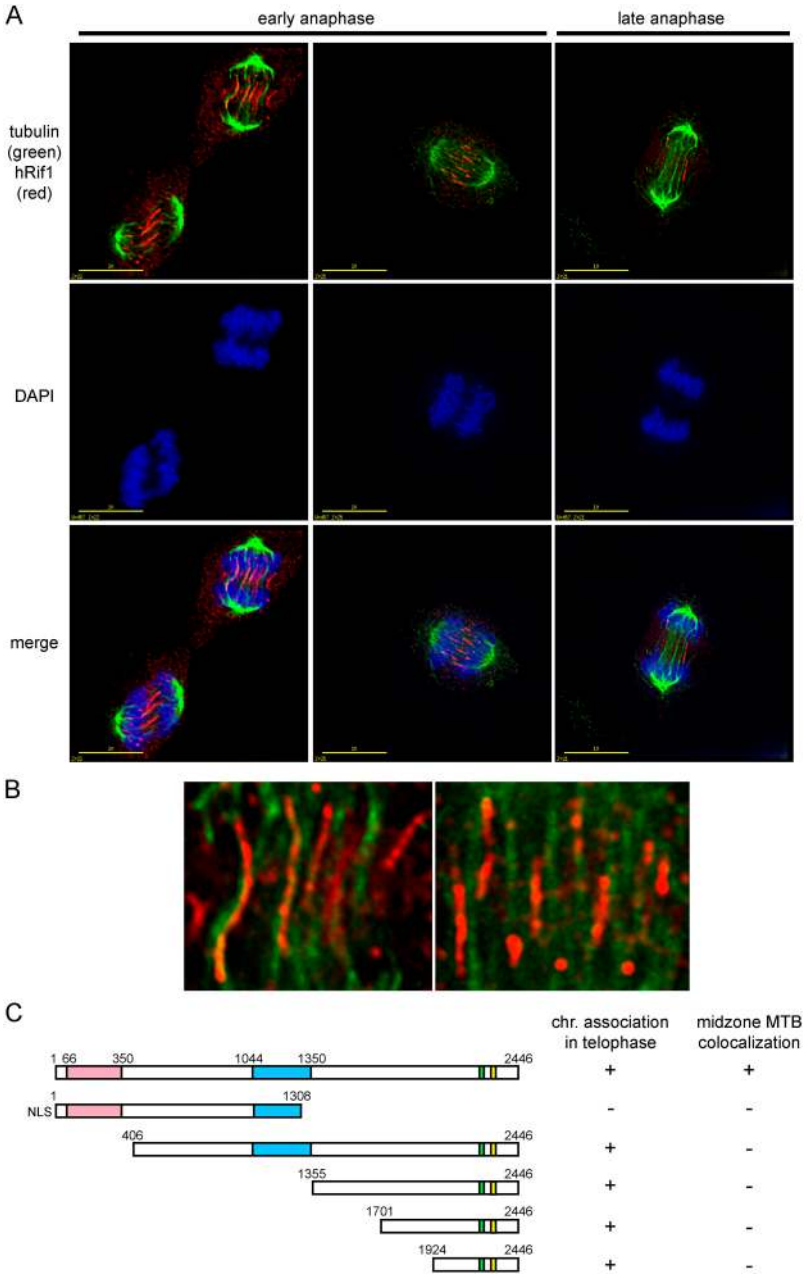

Figure 9. **hRif1 protein aligns along a subset of midzone microtubules at anaphase.** (A) Immunostaining of hRif1 in early anaphase and late anaphase LOX cells using hRif1 antibody (red), β-tubulin antibody (green), and DAPI (blue). Images were acquired with a Deltavision microscopy system as described in Fig. 8. (B) Enlarged images of early anaphase cells in A to show the alignment of hRif1 along microtubules. (C) Schematic representation of hRif1 deletion constructs used for analyses of telophase chromosome association and anaphase midzone microtubule colocalization. GFP-hRif1 deletion constructs were transfected into LOX cells and immunostaining was performed to determine their intracellular localization across the cell cycle. Bars, 10 μm.

at different cell cycle stages were further analyzed with dual immunostaining of hRif1 with the G2/M phase-specific protein cyclin B. Cyclin B synthesis starts in the last one third of S phase and reaches a maximum level in G2 and M phases (Gong et al., 1993). As shown in Fig. S4 (available at http://www.jcb.org/cgi/content/full/jcb.200408181/DC1), interphase cells that showed no staining of cyclin B, and which were judged on that basis to be in G1 or early- to mid-S phase, had much lower levels of hRif1 staining compared with interphase cells that had abundant cyclin B, which were in late S or G2 phase. Therefore, we conclude that the rise of hRif1 protein levels in the cell cycle occurs in late S or G2 phase.

Because *S. cerevisiae* Rif1p protein dynamically associates with telomeric chromatin through the cell cycle (Smith et al., 2003), we examined hRif1 localization at different cell cycle stages, using indirect immunofluorescence staining of endogenous hRif1 in LOX cells. In interphase cells, heterogeneous nuclear staining was observed for hRif1 protein. In metaphase cells, hRif1 was notably absent from the condensed chromosomes and instead was distributed widely throughout the rest of the cell volume. In contrast, in telophase cells all the visible hRif1 had become localized to the still condensed chromosomes (Fig. 8 B).

Interestingly, during early anaphase, a significant amount of hRif1 was observed to align along fiber-like structures that were coincident with (or minimally, overlapped with) a subset of the midzone microtubules located in between the two sets of separating chromosomes (Fig. 9, A and B). Furthermore, hRif1 was on more fibers in early anaphase cells than in late anaphase cells, indicating that this localization is a dynamic and regu-

lated process. Inspection of the separating chromosomes by deconvolution microscopy excluded the possibility that any anaphase bridges were present and that the hRif1 might have been associated with them. In addition, staining of anaphase cells with antibodies against 53BP1 does not show the same pattern (unpublished data). Hence, the hRif1 staining in this region was not attributable to association with chromosome damage sites. No localization to the midbody in cytokinesis was observed. The same pattern of cell cycle–dependent association of hRif1 with chromatin and midzone microtubules was corroborated by immunofluorescence staining of LOX cells and HeLa cells with two independent affinity-purified rabbit pAbs raised against two different hRif1 peptide epitopes using either PFA or methanol as fixation reagent, and also by transfecting LOX cells with a GFP-hRif1 fusion protein (Fig. S5, available at http://www.jcb.org/cgi/content/full/jcb.200408181/DC1). These different methods of hRif1 detection all gave identical results, confirming that this dynamic subcellular pattern was attributable to hRif1.

To identify regions of hRif1 that are required for the telophase reassociation with chromatin and the anaphase midzone microtubule colocalization, we constructed various hRif1 deletion constructs and fused them in-frame with the GFP. For the hRif1 deletion construct lacking the hRif1 cognate NLS, we added an SV40 T-antigen NLS to the NH_2 terminus (Fig. 9 C). Each deletion construct was then transfected into LOX cells and its cellular distribution examined by fluorescence microscopy. As shown in Fig. 9 C, the GFP fusion proteins containing full-length hRif1, hRif1$^{406\text{-}2446}$, hRif1$^{1355\text{-}2446}$, hRif1$^{1701\text{-}2446}$, and hRif1$^{1924\text{-}2446}$, but not (NLS)hRif1$^{1\text{-}1308}$, retained the ability to reassociate with chromatin at telophase. Hence, the 522–amino acid COOH-terminal region of hRif1 is sufficient for this property. In contrast, none of the deletion constructs tested colocalized with midzone microtubules in anaphase cells, suggesting that this colocalization requires both the NH_2-terminal conserved region (Fig. 1 A and Fig. 9 C, pink bars) and the COOH-terminal region of hRif1.

Discussion

Here, we have reported the identification and characterization of a human orthologue of Rif1 protein. The results provide evidence that the human Rif1 protein binds uncapped telomeres, is involved in the DNA damage response and associates with chromatin dynamically. Furthermore, we observed that hRif1 localizes along midzone microtubules specifically in early anaphase.

Findings made over the past several years have demonstrated that DNA damage responses and telomere maintenance cross paths. A growing list of proteins that have been defined by their roles in the repair of double-strand DNA breaks, such as Ku (Gravel et al., 1998; Hsu et al., 1999) and components of the MRN DNA damage complex (MRX complex in yeast; Zhu et al., 2000; Diede and Gottschling, 2001), are found at telomeres and are important for normal telomere maintenance in eukaryotes ranging from yeasts to humans. It is thought that the presence of the DNA damage machinery at telomeres may monitor and regulate telomerase action on telomeres, perhaps allowing cell cycle progression only after appropriate telomere replication and integrity are assured. Rif1 protein is different from the aforementioned DNA damage response proteins. In the budding yeast *S. cerevisiae*, scRif1p is regarded as being one of the integral members of the telomeric structural nucleoprotein complex, and to be recruited to telomeres by the telomere sequence-specific binding protein scRap1p to negatively regulate telomere length (Hardy et al., 1992). In contrast, we found that the human Rif1 counterpart has lost any detectable ability to associate with normal telomeres or regulate telomere length. Notably, the fission yeast and human Rif1 proteins have a role in responding to telomere aberrancies.

Human Rif1 protein responded to general DNA damage in human melanoma cells, as had also been reported by Silverman et al. (2004) for different cell lines. We found that depleting human cancer cells of Rif1 protein slowed their growth in culture. It is known that loss of the DNA damage repair protein Rad51 in vertebrate cells causes accumulation of chromosomal breaks and loss of cell viability (Tsuzuki et al., 1996; Sonoda et al., 1998). Therefore, we speculate that, like Rad51 and other DNA damage response proteins, hRif1 may be essential for repair of ongoing DNA damage and deficient hRif1 function may lead to accumulation of unrepaired DNA damage that impairs cell growth.

Evolution of Rif1

The results we observed with the human Rif1 orthologue provide a new perspective on the functions of Rif1 from an evolutionary point of view. In summary, from *S. cerevisiae* through *S. pombe* to humans, we see a progression in the tendency of Rif1 protein to associate to aberrant or damaged telomeres versus normal telomeres. In *S. cerevisiae*, scRif1p has been thought to be recruited to telomeres mainly through its interaction with the telomere binding protein scRap1p, and at least a subset of scRif1p protein is colocalized with telomeres across most if not the entire cell cycle (Mishra and Shore, 1999; Smith et al., 2003). However, inspection of the association of scRif1p and scRap1p proteins to telomeres during the cell cycle revealed that scRif1p has an association pattern clearly different from scRap1p (Smith et al., 2003): Notably, during S-phase, the telomere association of scRif1p reaches its maximum value in the cell cycle, whereas that of scRap1p decreases to its minimum value. Because scRap1p binds to duplex telomere DNA and provides a protective capping function, this pattern could reflect a role of scRif1p in responding to changes in telomere status. For example, scRif1p might be recruited to telomeres by other proteins when scRap1p there is low in order to provide a protective function for the Rap1-depleted telomeres, or scRif1p may send a signal to promote scRap1p association with telomeres. Consistent with our hypothesis that scRif1p has an elevated association with aberrant telomeres lacking scRap1p binding, it has also been observed that the relative level of association of scRif1p is slightly increased on the elongated and partially deregulated telomeres in a heteroallelic *tlc1-476A/TLC1 S. cerevisiae* strain, in which the association of scRap1p with telomeres was simultaneously found to be decreased (Smith et al., 2003). Although in *S. pombe*, spRif1p is found by

the chromatin immunoprecipitation method to be enriched at telomeres, and interacts with another duplex telomeric DNA binding protein Taz1 in a yeast two-hybrid assay, immunofluorescence studies show that it has a heterogeneous staining pattern in the nucleus and is not visualized at telomeres in wild-type cells (Kanoh and Ishikawa, 2001). Instead, *S. pombe* Rif1p is seen to translocate to telomeres only when the *S. pombe Rap1* gene is deleted. Because *S. pombe* Rap1p protein normally localizes to telomeres and its deletion results in greatly elongated telomeres (Chikashige and Hiraoka, 2001; Kanoh and Ishikawa, 2001), we propose that spRap1p provides capping function to telomeres in this yeast, and a substantial amount of *S. pombe* Rif1p only associates with aberrant telomeres that were uncapped. In human cells, hRif1 has lost any detectable association with normal telomeres or duplex telomeric DNA binding proteins TRF1, TRF2, or the human Rap1 orthologue hRap1, while keeping its function to respond to the aberrant telomeric DNA synthesized from a template mutant of telomerase RNA. Furthermore, hRif1 is involved in the general DNA damage response. These findings suggest that the cellular functions of hRif1 have diverged over evolution; however, when we overexpressed hRif1 in *S. cerevisiae*, we did observe interference in telomere length maintenance, which was specifically dependent on the presence of the yeast *Rif1* gene. Therefore, it is of great interest to understand what aspects of the Rif1 protein functions are conserved through evolution. It also remains to be elucidated whether Rif1p proteins in *S. cerevisiae* and *S. pombe* play a role in the response to at least some types of DNA damage.

Early anaphase–specific localization of hRif1 to midzone microtubules

While investigating the cell cycle–dependent subcellular distribution of hRif1, we have discovered that hRif1 localizes along a subset of the anaphase midzone microtubules, possibly decorating the midzone of these microtubules, or even forming fibers that overlap or coincide with these microtubules. The association was maximal in early anaphase, with progressively fewer microtubules showing this hRif1 association pattern as anaphase progressed and the two sets of chromosomes further separated. The data are consistent with hRif1 association with midzone microtubules occurring in anaphase A and becoming lost as cells enter anaphase B. Such microtubule association, combined with the overall cell cycle pattern of localization of hRif1, is novel and has not been reported for any other proteins. This subcellular localization behavior differs, for example, from that of chromosomal passenger proteins such as INCENP and other proteins of the aurora kinase complex. Like hRif1, these proteins are found on midzone microtubules in anaphase and in the nucleus in interphase but, unlike hRif1, localize specifically to centromeres in metaphase and to the midbody at cytokinesis (Cooke et al., 1987; Higuchi and Uhlmann, 2003). The behavior of hRif1 also distinguishes it from human chromatin protein Orc6, which is at kinetochores in metaphase, the midzone in anaphase, and at the midbody in cytokinesis (Prasanth et al., 2002), and from human chromatin repp86, which is nuclear in G1/S, centrosomal at the onset of mitosis, and localizes to the mitotic spindle in mitosis and to the midbody at cytokinesis (Heidebrecht et al., 2003).

We considered the possibility that hRif1 is being transported by microtubules to its subcellular targets. Because by the end of telophase, all the visible hRif1 colocalizes with the still-condensed chromosomes, specifically, hRif1 might be transported back to the chromosomes on microtubules. However, the fact that there is no accumulation of hRif1 on chromosomes even during late anaphase compared with early anaphase argues against this model. An attractive but untested possibility is that hRif1 is on microtubules where it serves to monitor mitotic exit and control the progress of anaphase. One observation consistent with this hypothesis is that in *S. cerevisiae*, chromosome loss rate increased ~7.5- and ~30-fold in *rif1* and *rif1rif2* mutants, respectively, compared with wild-type cells (Wotton and Shore, 1997). It was originally thought that this increase is caused directly by impaired telomere function, which potentially leads to telomere fusions and the instability of any resulting dicentric chromosomes. Our results now suggest that Rif1 proteins may in addition have a more direct role in monitoring mitotic exit and hence chromosome segregation, possibly by modulating microtubule properties. We did not observe a significant change in mitotic index in the LOX melanoma cells depleted of hRif1 by multiple siRNA constructs (unpublished data). Given that it is unknown over what range of concentrations hRif1 protein is functional in cells, it is feasible that the residual levels of hRif1 in these cells are still able to fulfill any function of monitoring mitotic exit. Thus, cells with a conditional hRif1 gene knockout may better address whether hRif1 affects mitotic progression. In addition to hRif1's midzone microtubule localization, it has been reported that human TRF1 localizes to the mitotic spindle during mitosis (Nakamura et al., 2001). Tankyrase, a TRF1 interacting protein, has also been observed at centrosomes in mitotic cells (Smith and de Lange, 1999). Therefore, the two seemingly unrelated structures, telomeres, and mitotic spindles, might have some intrinsic functional connections with each other. Understanding these potential interplays will help elucidate new aspects of the orchestration of chromosome integrity and cell cycle progression.

Materials and methods

Lentivirus infection

The lentiviral vector system was provided by D. Trono (University of Geneva, Geneva, Switzerland; Zufferey et al., 1997). Recombinant lentiviruses were generated by transfecting pMD.G, pCMVDR8.91, and a lentivector plasmid into 293T cells with lipofectamine 2000 (Invitrogen). Lentivirus-containing medium was harvested 48 and 72 h after transfection and filtered through 0.45-μm filters. For lentiviral infection, cells were incubated with virus-containing culture medium supplemented with 8 μg/ml polybrene for 8 h. For the cell growth experiments, 10^5 or 2×10^5 cells were seeded onto 10-cm culture plates 3 d after lentiviral infection, and the cell numbers were counted every 3 d.

Antibody production

Rabbit pAbs against peptide 2106-2123 NH_2-(GC)ESDILQEDHHTSQKVEEP-COOH (PAB2852) and peptide 2457-2472 NH_2-(GC)KNLQSRWRSPSH-ENSI-COOH (PAB2857) of hRif1 were generated (Bio-Synthesis, Inc.) and affinity-purified against their corresponding peptide (Rockland Immunochemicals).

RNA interference

Lentiviral hairpin siRNA expression vectors were constructed as described previously (Li et al., 2004). The target sequences for the siRNA are: hRif1-GACTCACATTTCCAGTCAA(6037), GCTGAGTAGTGCTGCTCTACA (6038), GGAGAGACGCATTCTGCTG(6039), GAGGCAGTGAGGTGG-GCAA(6041), GCTCTGGAGATGGGAATGCCA(6042), GAGAAAC-CAGGTTCTGAAG(6053), GATGAAATCTCATCACCTG(6054); hRap1-GATTTCATCTCCACGCAGTAC(6044); TRF1-GAATATTTGGTGATCCAAA (6055), GGAACATGACAAACTTCATGA(6059); TRF2-GAGGATGAACTG-TTTCAAG(6056), GCTGCTGTCATTATTTGTATC(6061). For cell growth analysis, HT1080 cells and LOX cells were infected with lentiviral hairpin siRNA constructs at >95% efficiency of infection as indicated by a GFP expressed from the same lentiviral vector. For telomere length analysis and immunofluorescent staining, the GFP gene in the lentiviral hairpin siRNA vector was replaced by a puromycin resistance gene. Cells were infected with corresponding lentiviruses and maintained in puromycin selection medium.

RNA analysis

Total RNA was extracted using TRIzol reagent (Invitrogen). mRNA was isolated using FastTrack 2.0 kit (Invitrogen). The 5′- and 3′-end of hRif1 cDNA was determined by the 5′- and 3′-RACE system (Invitrogen). hRif1 cDNA was amplified by PCR of first-strand cDNA synthesized with the SuperScript first-strand synthesis system for RT-PCR (Invitrogen).

For Northern blot analysis of hRif1, 2 μg of mRNAs or 40 μg of total RNAs were treated with glyoxal (Sigma-Aldrich), electrophoresed on a 0.8% or a 1% agarose gel, transferred to Hybond-NX membrane, and hybridized with hRif1 or β-actin probes labeled with α-[^{32}P]-dCTP using RediPrime II kit (Amersham Biosciences). The blots were analyzed by phosphorimaging and quantified with the ImageQuant software (Molecular Dynamics).

Immunoprecipitation and Western blot analysis

Cells were lysed in NP-40 lysis buffer (50 mM Tris, pH 8.0, 150 mM NaCl, 2 mM EDTA, 1% NP-40, and protease inhibitors). After 20 min on ice, the lysates were centrifuged at 14,000 rpm for 10 min and precleared by incubation with 40 μl of protein A– or G–Sepharose beads (Sigma-Aldrich) at 4°C for 30 min to obtain the whole cell extracts for immunoprecipitation. To examine the interaction of hRif1 with TRF1, TRF2, and hRap1, coimmunoprecipitation of hRif1 with the endogenous TRF1, TRF2, and hRap1 proteins, as well as with transiently transfected myc-tagged TRF1, TRF2, and hRap1 proteins were performed. In brief, 1mg of total protein of each whole cell extract was incubated with antibodies against TRF1 (Novus), TRF2 (BD Transduction Laboratories) and hRap1 (Bethyl Laboratories) and protein A or G beads (Sigma-Aldrich) in a total volume of 500 μl for 4 h at 4°C. The beads were washed three times with lysis buffer, resuspended in Laemmli loading buffer, and analyzed by SDS-PAGE and Western blotting. For immunoprecipitation of hRif1 with ectopically expressed myc-tagged TRF1, TRF2, and hRap1 proteins, myc-tagged TRF1, TRF2, and hRap1 expression constructs were transfected into 293 cells using lipofectamine 2000 (Invitrogen). Typically, >90% of cells could be transfected. Whole cell extracts were made 2 d after transfection, and immunoprecipitation was performed using anti-myc antibody 9E10 (Covance).

For Western blot analysis, PAB2857 were used to detect hRif1 protein. The same blot was probed with anti–α-tubulin (Sigma-Aldrich) antibody as loading controls.

Indirect immunofluorescence microscopy

Cells were grown on glass coverslips, fixed with 2% PFA in PBS, and permeabilized with 0.5% NP-40 in PBS. Immunostaining was performed using primary antibodies against β-tubulin (Sigma-Aldrich), TRF1 (Novus Biologicals), TRF2 (BD Transduction Laboratories), hRap1 (Bethyl Laboratories), 53BP1 (BD Transduction Laboratories), cyclin B (BD Transduction Laboratories), and two rabbit polyclonal peptide antibodies against hRif1, followed by appropriate secondary antibodies conjugated with Alexa Fluor 488 or 568 (Molecular Probes). DNA was visualized with 0.2 μg/ml DAPI.

Unless otherwise pointed out, all images were analyzed using a Deltavision Restoration Microscopy system (Applied Precision) with a 60× objective and 1.5× magnifier. Images were acquired with the Deltavision SoftWorx resolve3D capture program and collected as a stack of 0.2-μm increments in the z axis. After deconvolution, images were viewed either with the Quick Projection option or as a single section on the z axis.

Synchronization of T24 cells

Human bladder carcinoma T24 cells were synchronized at G0/G1 by contact inhibition according to established protocols (Chen et al., 1996). In brief, cells were seeded onto 10-cm culture plates. Fresh medium was added to cultured cells every other day. After at least 7 d of confluence, the cells were split onto 10-cm culture plates at a concentration of 10^6 cells per plate in fresh medium. Three plates were collected at each time point: two for Western blot analysis and one for FACS analysis of DNA content using propidium iodide staining.

GenBank accession No.

The GenBank/EMBL/DDBL accession nos. for the hRif1 cDNA reported in this article are AY727910–AY727913.

Online supplemental material

Fig. S1 shows the amino acid sequence of hRif1. Fig. S2 shows telomere length analysis of HT1080 human fibrosarcoma lines depleted of hRif1 protein. Fig. S3 shows telomere length analysis in *wild-type*, Δ*rif1*, Δ*rif2*, and Δ*rif1*Δ*rif2* mutant *S. cerevisiae* strains overexpressing hRif1 protein or the vector-alone control. Fig. S4 shows that a higher level of hRif1 protein is found in interphase LOX melanoma cells expressing cyclin B. Fig. S5 shows in LOX melanoma cells the midzone microtubule localization of the transfected GFP-hRif1 fusion protein fixed with PFA and the endogenous hRif1 protein fixed with methanol. Online supplemental material is available at http://www.jcb.org/cgi/content/full/jcb.200408181/DC1.

We thank Shang Li (UCSF) for the lentiviral telomerase RNA expression construct and Dan Levy (UCSF) for yEHB11188 strain. We thank Jeff Seidel, Shivani Nautiyal, Tanya Williams, and Dan Levy for critical reading of the manuscript. We are grateful to Wallace Marshall (UCSF) for providing the Deltavision Microscope.

This work was supported by National Institutes of Health grant CA096840 to E.H. Blackburn. L. Xu was supported by a Susan G. Komen postdoctoral fellowship and an National Institutes of Health postdoctoral training grant.

Submitted: 31 August 2004
Accepted: 28 October 2004

References

Adams, I.R., and A. McLaren. 2004. Identification and characterisation of mRif1: a mouse telomere-associated protein highly expressed in germ cells and embryo-derived pluripotent stem cells. *Dev. Dyn.* 229:733–744.

Bakkenist, C.J., and M.B. Kastan. 2003. DNA damage activates ATM through intermolecular autophosphorylation and dimer dissociation. *Nature.* 421: 499–506.

Blackburn, E.H. 2000. The end of the (DNA) line. *Nat. Struct. Biol.* 7:847–850.

Blackburn, E.H. 2001. Switching and signaling at the telomere. *Cell.* 106: 661–673.

Broccoli, D., A. Smogorzewska, L. Chong, and T. de Lange. 1997. Human telomeres contain two distinct Myb-related proteins, TRF1 and TRF2. *Nat. Genet.* 17:231–235.

Bunz, F., A. Dutriaux, C. Lengauer, T. Waldman, S. Zhou, J.P. Brown, J.M. Sedivy, K.W. Kinzler, and B. Vogelstein. 1998. Requirement for p53 and p21 to sustain G2 arrest after DNA damage. *Science.* 282:1497–1501.

Chen, Y., A.A. Farmer, C.F. Chen, D.C. Jones, P.L. Chen, and W.H. Lee. 1996. BRCA1 is a 220-kDa nuclear phosphoprotein that is expressed and phosphorylated in a cell cycle-dependent manner. *Cancer Res.* 56:3168–3172.

Chikashige, Y., and Y. Hiraoka. 2001. Telomere binding of the Rap1 protein is required for meiosis in fission yeast. *Curr. Biol.* 11:1618–1623.

Cho, R.J., M.J. Campbell, E.A. Winzeler, L. Steinmetz, A. Conway, L. Wodicka, T.G. Wolfsberg, A.E. Gabrielian, D. Landsman, D.J. Lockhart, and R.W. Davis. 1998. A genome-wide transcriptional analysis of the mitotic cell cycle. *Mol. Cell.* 2:65–73.

Cooke, C.A., M.M. Heck, and W.C. Earnshaw. 1987. The inner centromere protein (INCENP) antigens: movement from inner centromere to midbody during mitosis. *J. Cell Biol.* 105:2053–2067.

Cooper, J.P., E.R. Nimmo, R.C. Allshire, and T.R. Cech. 1997. Regulation of telomere length and function by a Myb-domain protein in fission yeast. *Nature.* 385:744–747.

Diede, S.J., and D.E. Gottschling. 2001. Exonuclease activity is required for sequence addition and Cdc13p loading at a de novo telomere. *Curr. Biol.* 11:1336–1340.

Gong, J., F. Traganos, and Z. Darzynkiewicz. 1993. Simultaneous analysis of

cell cycle kinetics at two different DNA ploidy levels based on DNA content and cyclin B measurements. *Cancer Res.* 53:5096–5099.

Gravel, S., M. Larrivee, P. Labrecque, and R.J. Wellinger. 1998. Yeast Ku as a regulator of chromosomal DNA end structure. *Science.* 280:741–744.

Greider, C.W., and E.H. Blackburn. 1985. Identification of a specific telomere terminal transferase activity in Tetrahymena extracts. *Cell.* 43:405–413.

Hardy, C.F., L. Sussel, and D. Shore. 1992. A RAP1-interacting protein involved in transcriptional silencing and telomere length regulation. *Genes Dev.* 6:801–814.

Heidebrecht, H.J., S. Adam-Klages, M. Szczepanowski, M. Pollmann, F. Buck, E. Endl, M.L. Kruse, P. Rudolph, and R. Parwaresch. 2003. repp86: A human protein associated in the progression of mitosis. *Mol. Cancer Res.* 1:271–279.

Higuchi, T., and F. Uhlmann. 2003. Cell cycle: passenger acrobatics. *Nature.* 426:780–781.

Hsu, H.L., D. Gilley, E.H. Blackburn, and D.J. Chen. 1999. Ku is associated with the telomere in mammals. *Proc. Natl. Acad. Sci. USA.* 96:12454–12458.

Kanoh, J., and F. Ishikawa. 2001. spRap1 and spRif1, recruited to telomeres by Taz1, are essential for telomere function in fission yeast. *Curr. Biol.* 11: 1624–1630.

Karlseder, J., D. Broccoli, Y. Dai, S. Hardy, and T. de Lange. 1999. p53- and ATM-dependent apoptosis induced by telomeres lacking TRF2. *Science.* 283:1321–1325.

Kirk, K.E., B.P. Harmon, I.K. Reichardt, J.W. Sedat, and E.H. Blackburn. 1997. Block in anaphase chromosome separation caused by a telomerase template mutation. *Science.* 275:1478–1481.

Levy, D.L. and E.H. Blackburn. 2004. Counting of Rif1p and Rif2p on yeast telomeres regulates telomere length. *Mol. Cell. Biol*. 24:10857–10867.

Li, B., and T. de Lange. 2003. Rap1 affects the length and heterogeneity of human telomeres. *Mol. Biol. Cell.* 14:5060–5068.

Li, B., S. Oestreich, and T. de Lange. 2000. Identification of human Rap1: implications for telomere evolution. *Cell.* 101:471–483.

Li, S., J.E. Rosenberg, A.A. Donjacour, I.L. Botchkina, Y.K. Hom, G.R. Cunha, and E.H. Blackburn. 2004. Rapid inhibition of cancer cell growth induced by lentiviral delivery and expression of mutant-template telomerase RNA and anti-telomerase short-interfering RNA. *Cancer Res.* 64: 4833–4840.

Marusic, L., M. Anton, A. Tidy, P. Wang, B. Villeponteau, and S. Bacchetti. 1997. Reprogramming of telomerase by expression of mutant telomerase RNA template in human cells leads to altered telomeres that correlate with reduced cell viability. *Mol. Cell. Biol.* 17:6394–6401.

Mishra, K., and D. Shore. 1999. Yeast Ku protein plays a direct role in telomeric silencing and counteracts inhibition by rif proteins. *Curr. Biol.* 9:1123–1126.

Nakamura, M., X.Z. Zhou, S. Kishi, I. Kosugi, Y. Tsutsui, and K.P. Lu. 2001. A specific interaction between the telomeric protein Pin2/TRF1 and the mitotic spindle. *Curr. Biol.* 11:1512–1516.

Prasanth, S.G., K.V. Prasanth, and B. Stillman. 2002. Orc6 involved in DNA replication, chromosome segregation, and cytokinesis. *Science.* 297: 1026–1031.

Rappold, I., K. Iwabuchi, T. Date, and J. Chen. 2001. Tumor suppressor p53 binding protein 1 (53BP1) is involved in DNA damage-signaling pathways. *J. Cell Biol.* 153:613–620.

Schultz, L.B., N.H. Chehab, A. Malikzay, and T.D. Halazonetis. 2000. p53 binding protein 1 (53BP1) is an early participant in the cellular response to DNA double-strand breaks. *J. Cell Biol.* 151:1381–1390.

Silverman, J., H. Takai, S.B.C. Buonomo, F. Eisenhaber, and T. de Lange. 2004. Human Rif1, ortholog of a yeast telomeric protein, is regulated by ATM and 53BP1 and functions in the S-phase checkpoint. *Genes Dev.* 18:2108–2119.

Smith, C.D., D.L. Smith, J.L. DeRisi, and E.H. Blackburn. 2003. Telomeric protein distributions and remodeling through the cell cycle in *Saccharomyces cerevisiae*. *Mol. Biol. Cell.* 14:556–570.

Smith, S., and T. de Lange. 1999. Cell cycle dependent localization of the telomeric PARP, tankyrase, to nuclear pore complexes and centrosomes. *J. Cell Sci.* 112:3649–3656.z

Smogorzewska, A., and T. De Lange. 2004. Regulation of telomerase by telomeric proteins. *Annu. Rev. Biochem.* 73:177–208.

Sonoda, E., M.S. Sasaki, J.M. Buerstedde, O. Bezzubova, A. Shinohara, H. Ogawa, M. Takata, Y. Yamaguchi-Iwai, and S. Takeda. 1998. Rad51-deficient vertebrate cells accumulate chromosomal breaks prior to cell death. *EMBO J.* 17:598–608.

Takai, H., A. Smogorzewska, and T. de Lange. 2003. DNA damage foci at dysfunctional telomeres. *Curr. Biol.* 13:1549–1556.

Tsuzuki, T., Y. Fujii, K. Sakumi, Y. Tominaga, K. Nakao, M. Sekiguchi, A. Matsushiro, Y. Yoshimura, and T. Morita. 1996. Targeted disruption of the Rad51 gene leads to lethality in embryonic mice. *Proc. Natl. Acad. Sci. USA.* 93:6236–6240.

van Steensel, B., A. Smogorzewska, and T. de Lange. 1998. TRF2 protects human telomeres from end-to-end fusions. *Cell.* 92:401–413.

Wotton, D., and D. Shore. 1997. A novel Rap1p-interacting factor, Rif2p, cooperates with Rif1p to regulate telomere length in *Saccharomyces cerevisiae*. *Genes Dev.* 11:748–760.

Zhu, X.D., B. Kuster, M. Mann, J.H. Petrini, and T. de Lange. 2000. Cell-cycle-regulated association of RAD50/MRE11/NBS1 with TRF2 and human telomeres. *Nat. Genet.* 25:347–352.

Zufferey, R., D. Nagy, R.J. Mandel, L. Naldini, and D. Trono. 1997. Multiply attenuated lentiviral vector achieves efficient gene delivery in vivo. *Nat. Biotechnol.* 15:871–875.